energies

MDPI

Article

Power Flow Control Using Series Voltage Source Converters in Distribution Grids

Guilherme Gonçalves Pinheiro [1,*], Carlos Henrique da Silva [2], Bruno P. B. Guimarães [1], Robson Bauwelz Gonzatti [1], Rondineli Rodrigues Pereira [1], Wilson Cesar Sant'Ana [3], Germano Lambert-Torres [3,*] and Joselino Santana-Filho [4]

1 Institute of Engineering and Information Technology (IESTI), Federal University of Itajuba, Itajuba 37500-903, Brazil; brunoguimara@unifei.edu.br (B.P.B.G.); rbgonzatti@unifei.edu.br (R.B.G.); rondineli@unifei.edu.br (R.R.P.)
2 Electrical Engineering Department, Federal University of Ouro Preto, Joao Monlevade 35931-008, Brazil; carlos.silva@ufop.edu.br
3 Gnarus Institute, Itajuba 37500-052, Brazil; wilson_santana@ieee.org
4 Engineering Department, EDP Sao Paulo, Sao Paulo 08820-460, Brazil; joselino.filho@edp.com
* Correspondence: guilhermegpinheiro@unifei.edu.br (G.G.P.); germanoltorres@gmail.com (G.L.-T.)

Abstract: This study presents an application for a series VSC (voltage source converter) in distribution grids for power flow management. Series devices have been widely studied for FACTS (flexible AC transmission systems), however, more recently these devices have gained increased interest in applications for loading balance in medium voltage distribution grids. As the number of distributed generation (DG) units increases, increasing the capacity and reliability of distribution grids while maximizing the benefits of installed DGs and loading behavior is an ever more important task. In this paper, we describe a test system and control proposals for a practical application of series converters interconnecting two distribution feeders at 13.8 kV under load variation disturbances. This approach provides solutions when installed at the end of distribution lines by interconnecting two feeders, resulting in capacity increases in the feeders without needing grid reconfigurations using a small-rated series VSC.

Keywords: contingency management; meshed grids; resilient AC distribution systems; power routers; smart grids

Citation: Pinheiro, G.G.; da Silva, C.H.; Guimarães, B.P.B.; Gonzatti, R.B.; Pereira, R.R.; Sant'Ana, W.C.; Lambert-Torres, G.; Santana-Filho, J. Power Flow Control Using Series Voltage Source Converters in Distribution Grids. *Energies* **2022**, *15*, 3337. https://doi.org/10.3390/en15093337

Academic Editor: Ferdinanda Ponci

Received: 11 March 2022
Accepted: 28 April 2022
Published: 4 May 2022

1. Introduction

Power quality issues and contingency management techniques have been a constant challenge over the past 30 years for transmission systems and more recently for distribution grids [1–3]. Traditional techniques for mitigating contingencies and balancing loads in power systems include grid reconfigurations, new investments in transmission lines, installing new substations, etc., and have promised reduced technical losses and increased distribution reliability and capacity. However, these are practices that require high-cost investments even though nearby lines sometimes are often idle, while others are overloaded.

Instead of installing new infrastructures to increase capacities and power transfer capabilities [4], power flow manipulation is traditionally achieved using phase-shifting transformers (PSTs) in transmission systems. Modernization using flexible AC transmission systems (FACTS) derived technologies has resulted in changes to traditional methods to improve the capacity of distribution grids. Distribution grid modernization is an essential challenge when seeking to provide more resilient systems as transmission grids are improved. This may include using smart converters, digital protection schemes, or remote operations.

It is known that FACTS allow existing grids to be used closer to their thermal capacities and economic limits, without drawbacks in stability [5], resulting in better energy use. As explained in [6], power electronic solutions for distribution grid applications are technologically analogous to modern FACTS with voltage source converters (VSC) and are known as RACDS (resilient AC distribution systems).

The series VSC of this study is considered an active tool, which can be applied to the smart grid concept. The smart grid concept can be defined as the modernization and use of active tools, with control capabilities and telecommunication architectures, in existing power systems [7]. This allows efficient energy utilization (e.g., in grids with bidirectional power flow as in presence of DGs) when devices are embedded with intelligent algorithms, sometimes controlled autonomously or remotely.

In fully supervised systems, the smart grid philosophy also includes the coordinated use of many types of RACDS devices and ensures improvements in congestion, thus reducing technical losses and the duration and frequency of outages. Furthermore, the authors of [8] consider a smart grid as the better use of devices and sensors spread throughout the grid.

Distribution grids are traditionally designed using radial topology for unidirectional power flow. Nevertheless, the increasing use of distributed renewable energy resources has drawn the attention of researchers to management solutions for smart load flow behavior, thus guaranteeing increases in the capacity and reliability of these types of power systems for solving voltage and overload problems. Nowadays the compensation approach using series converters has spurred innovations in new technologies while creating challenges for solving many power quality drawbacks associated with the increased investment demands in distribution grids.

Series VSCs have been widely investigated in the power electronics fields, like series active power filters, dynamic voltage restorers (DVRs), and static synchronous series compensators (SSSCs). SSSCs inject an independently controlled voltage in quadrature with the line current and can be used for impedance compensation in long transmission lines, and need only reactive power exchanges with the line without a DC source. On the other hand, to have more degrees of freedom and to control both active and reactive power flow with a series compensator in a meshed grid, either energy storage or a path to receive active power from one of the feeders is required.

The main trends in recent research related to solutions for power flow controllers, or power routers, are listed below. References [9,10] present the features and experimental results for meshed grids using unified power flow controllers (UPFCs) applied to distribution systems for reducing technical losses and providing voltage regulation. A study on the benefits of using looping radial distribution systems is discussed in reference [11], where a multilevel cascaded H-bridge series converter connecting feeders from different substations was used. Furthermore, Ref. [12] shows the power system behavior when using closed loops in radial systems for distribution and transmission levels, with analysis considering the loop current path for variances in line impedances.

Reference [13] highlighted challenges and limitations in simulations using additional series converters in short-circuit applications with resonant controllers for medium voltage systems. The drawbacks presented in the study were that the converter needed to impose a voltage at the nominal value in the grid. Furthermore, Ref. [14] presented a technique for turning off the IGBTs (i.e., using freewheeling diodes) during a short circuit and thus, blocking the current flowing through the interconnection during a fault, and Ref. [15] presented a simulation for a series converter to substitute the phase shift transformers to control the power flow and mitigate short circuiting.

A multilevel cascaded H-bridge converter called a distribution static synchronous series compensator (DSSSC) was presented in [16], along with the simulation results for a case study at 20 kV. The study also presented the experimental low-voltage results and offered proposals for control strategies. References [17,18] presented topologies for

series AC-AC converters, called controllable network transformers (CNTs) and the authors of [19,20] presented a compact dynamic phase angle regulator (CD-PAR).

A hybrid solution is presented in [21,22], using a series-series VSC topology with a shunt variable capacitor for transmission and distribution systems. These publications present simulations and selectable control modes for each system behavior and propose an optimal dispatch algorithm for power flow control.

References [23,24] comment on loop power flow controllers and propose a back-to-back (BTB) converter for a case study for a 6.6 kV level distribution voltage. Additionally, Refs. [25,26] present an autonomous control technique for power flow controllers that tracks the best power transfer to minimize losses using information from terminal voltages with a BTB converter.

About the presented AC-AC converters, Ref. [26] presented drawbacks for a series VSC solution emphasizing fault sensitive problems and the limited lifetime of the DC-link capacitance, and thus propose a buck-type AC-AC converter called a direct power flow controller.

Back-to-back converters interconnected to distribution feeders seem to be the best alternative for this type of application [27], i.e., this equipment makes use of PQ power transfer between the feeders, resulting in reactive compensation, consequently improving the terminal voltage and in general improving the overall power quality. However, this bulky solution is complex and more costly than series VSCs because full-rated multilevel converters for making the interconnections are needed, e.g., for a 1 MVA power transfer, two 1 MVA DC-AC converters are needed.

One should note that distribution grids do not have a large variation in the phase angle difference between close feeders when they come from the same main source [28]. Distribution lines are relatively short compared to transmission systems. Instead of using a back-to-back converter, a small-rated series VSC could provide a low-cost approach because only a fraction of the system voltage is needed for loading flow manipulation, even though this approach is not as flexible as the BTB converter [29].

Furthermore, these solutions can balance power between the future distribution of meshed feeders, and consequently improve power quality, while reducing technical losses. In [28], their application demonstrates that any changes in the power flow through any grid lead to improvements in the reactive power requirements from the main generators.

The approach allows radial distribution grids to be converted into meshed grids. This results in a controlled and secured way of improving operation in real time and during contingencies. Series devices have fewer commercial applications than shunt devices (not as effective for flow control), and in many cases, the series VSC alone can provide features for effective loading balance management [6]. Additionally, series VSC is more vulnerable to fault currents [30,31]. The biggest challenge when inserting a series converter into an electrical system is that it must be able to make smart decisions or be removed and protected in case of either a short circuit or a power outage.

This work demonstrates a solution of an active tool that contributes to independent control and transfer of active and reactive powers between distribution feeders. Instead of the use of a bulky back-to-back converter, the small-rated series VSC can be a low-cost solution for the same application. Figure 1 shows the topology of the developed series real-time power flow controller that was built and applied in a 13.8 kV test system. The control system, based on the MSRF (modified synchronous reference frame), was implemented in a TMS320F28335 DSP (digital signal processor).

The power circuit comprises an IGBT-based H-bridge converter connected in series with the distribution lines using a coupling transformer with a diode rectifier supplying the DC-link for each phase. Every phase has its own controller and power circuit, resulting in a modular design that can be arranged for a single or three-phase system. The proposed topology can perform:

1. Bidirectional active power transfer;
2. Bidirectional reactive power transfer;

3. Voltage imbalance;
4. Harmonic isolation;
5. Protection scheme.

Several applications of the proposed system can be mentioned, although not covered completely in this publication due to lack of space. Regarding the embedded protection scheme, the solution can quickly protect the converter in surges (over-voltages and over-currents) using a thyristor-based system that removes the converter during either a fault or an outage, which will be presented and detailed in a future publication.

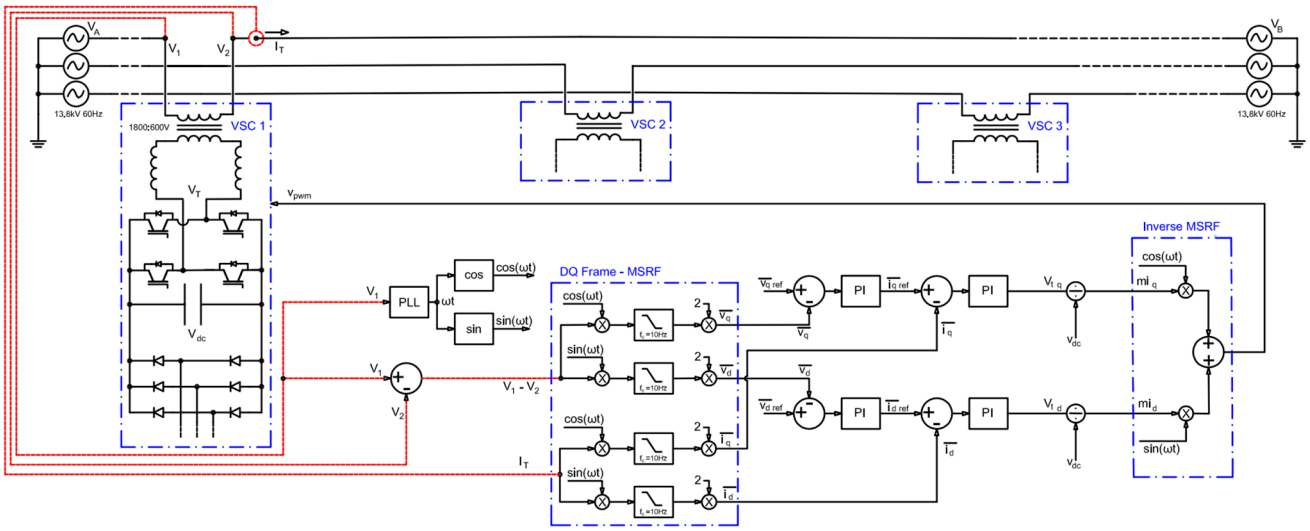

Figure 1. Modular three-phase series VSC connecting two feeders and the control system.

With respect to the harmonic isolation feature, the proposed series VSC could provide improvements in power quality as shown in [32]. The converter is also a series active power filter that can harmonically isolate both feeders, keeping the system, from the harmonic point of view, as it was before the interconnection. This is achieved by transferring power between the interconnected feeders exclusively at the fundamental frequency, providing improvements in terminal voltage profiles. Still, this feature is not the main focus of the present article.

In presence of renewable energies or DGs, fluctuations of terminal voltages are commonly caused by the varying active power injected by DGs at the end of long feeders. In this scenario, the equipment can use the power generated by renewables for better active power distribution between feeders, consequently providing mitigation of the voltage fluctuations and over-voltages.

Another application is for reactive power control in situations where there are fixed capacitor banks installed in some of the feeders. The excess of reactive power from existing capacitor banks can be transferred to another branch that is interconnected by the converter, where, at certain times, there is a need for reactive compensation.

Moreover, as distribution systems are unbalanced, the series VSC is composed of three single-phase converters and every phase has its own controller and power circuit (based on the MSRF technique applied in independent single-phase converters), which provides the features for voltage unbalance mitigation.

Thus, focusing on both active and reactive power transfer, this paper provides contributions on modeling fundamentals, control proposals, and the practical results for a series VSC used in 13.8 kV laboratory and field tests.

Furthermore, the next sections show firstly the discussion about the problem formulation and operating challenges regarding the use of series converters application in distribution grids. Finally, it presents the control system and experimental results.

2. Formulation of the Problem

This section will highlight some relevant aspects regarding the strategic changes from a radial to a meshed distribution grid by permanently interconnecting two feeders at the end of their lines, based on reference [28].

Traditionally, distribution grids do not operate in a permanent loop or ring. Figure 2 shows a typical distribution system. A well-known operating procedure commonly used in distribution grids is when two feeders are connected in parallel (indicated in Figure 2 as a normally open switch) for a short time and one of the feeders is removed at the beginning. This is an operating procedure used for maintenance, and it interrupts only a small section of the whole system. This operating procedure is a momentary reconfiguration that prevents many loads from not being supplied for long periods during strategic operations or maintenance.

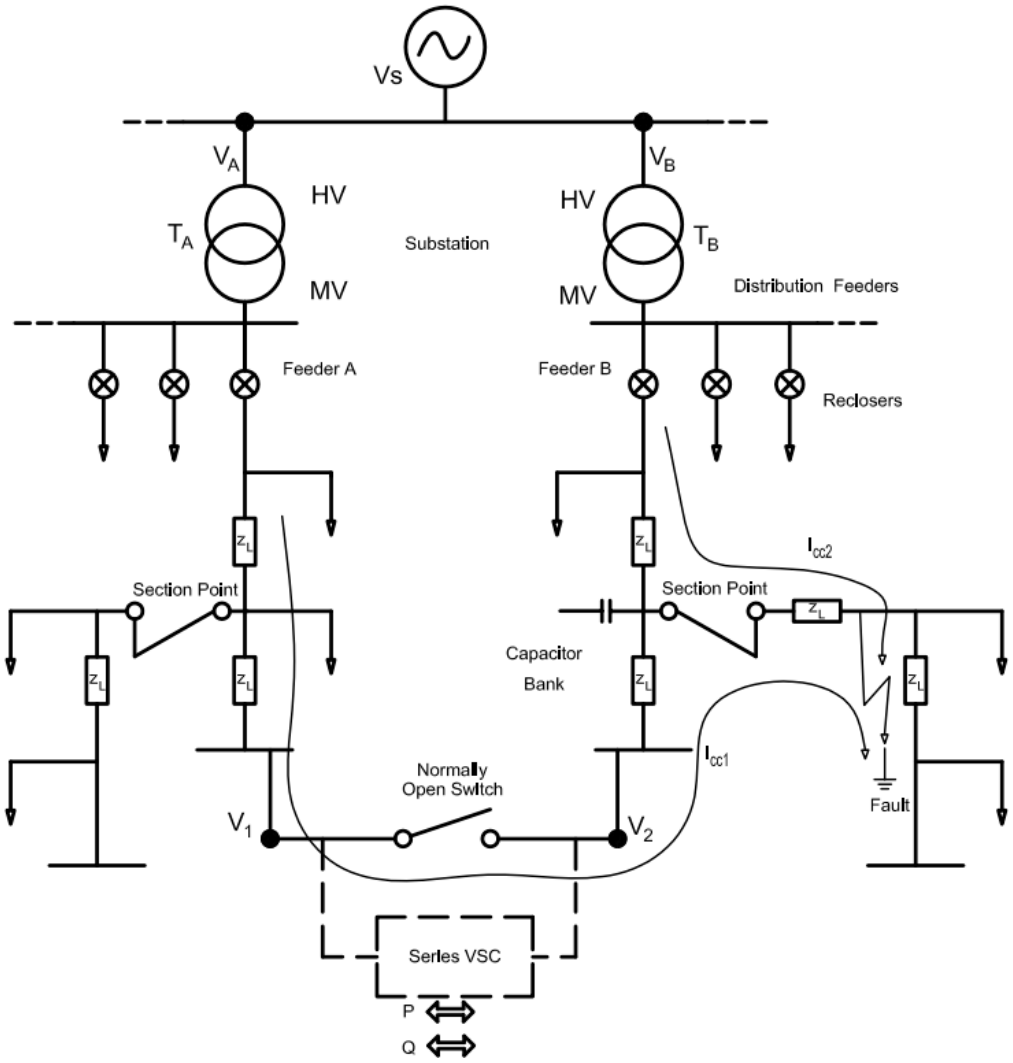

Figure 2. Typical distribution system.

Distribution systems are commonly radial and overhead. In some cases, the normally open switch (Figure 2) represents a backup source for reducing interruption times. A strategic rule for ensuring reliability is that at least two feeders at each consumption point are needed [28]. However, nearby lines are sometimes nearly empty while others are overloaded.

Furthermore, it is common to use reclosers installed at strategical places in distribution systems, sometimes using remote command, to prevent long outages at critical loads when maintenance is needed and/or fault conditions occur. It is well known that distribution

lines have a small phase rotation [28,33], since it comes from the same main voltage source, and since it has the same configuration as the substation's step-down transformers, allowing one to permanently operate this system in a meshed configuration. Nevertheless, the impact on the short-circuit level does not allow for a permanent grid reconfiguration this way.

Figure 2 shows the flow of short-circuit currents. Depending on the location of the fault during a phase-to-ground short circuit, the voltage over the converter can reach grid-rated voltage values, which requires an effective protection system for a small-rated topology.

It should be noted that for meshed grids the short-circuit currents flow from both feeders, and this current in the indicated section point can be more damaging (i.e., $I_{cc} = I_{cc1} + I_{cc2}$) for local protections. Through the interconnected ring (location of the installed converter) the short-circuit currents do not rise like they do in the indicated fault section point. Therefore, in terms of protection, this condition is less damaging to the series converter than at the section point. Regarding the short-circuit behavior, a series converter may be applied with an appropriate protection scheme, as in [31,34].

In distribution systems, it is common to use a series of step-up transformers for relatively long distribution lines to compensate for distance voltage drops. In the same way, capacitors are applied for reactive power compensation even knowing that the reactive power flow is less effective in distribution lines than in transmission systems for voltage improvements.

Reactive power flows are effective in transmission due to the high *X/R* ratio. In distribution systems, the *X/R* ratio is close to a unity value, and the best place for reactive power injection is close to the loads. Thus, in distribution systems the power factor correction helps alleviate the VAr flow, which increases the ability of circuits to transport more active power.

Furthermore, it is known that the system stability concept is the ability to remain in stable operating conditions (acceptable voltages and power flow) even after a small (dynamic stability) or large disturbance (transient stability). During large disturbances, as explained above, the protection scheme removes the converter from the system and both feeders return to the radial configuration. With respect to the dynamic stability issues, the typical phase difference between the feeders where the proposed solution may be installed is small (about 3 to 5 degrees) and the small-rated low-voltage converter is able to impose a voltage to P&Q manipulation up to 11 degrees i.e., the converter's power rating is a small fraction of the power transfer capacity which reduces the capacity of operation during large disturbances. This phase angle difference is a value far away from the system stability limit, which is 90 degrees [35]. Since the purpose of this equipment is to manipulate power only during relatively small disturbances, the converter will always operate in a stable range without reaching the dynamic stability limits. In addition, the results presented show the behavior of the converter during load disturbances, which showed that after load variations (demonstrating amplitude and angle variations during the converter operation), the system returns to stable conditions, proving its behavior within the stability margins.

Finally, the series converter can be installed to replace (or in parallel to) the *normally open switch*, indicated in Figure 2, and can provide real-time active and reactive power flow control, providing load balance between feeders, voltage profile improvements, increased load capacity, and allowing for distribution grids to be automated.

3. Modelling

To analyze the distribution system that will apply a series converter, one must define a coherent dynamic representation. For large systems, it is common to use iterative methods for solving the load flow, especially in meshed grids. In distribution systems, distributed parameters or pi-sections modeling is not needed for short distances less than 80 km. Thus, one approach for this modeling can be achieved with a series impedance ($R + jX$), and shunt conductance can be disregarded [28].

For dynamic representation, the equations that describe the dynamics of the system can be linearized for analysis even if the power system formulation is nonlinear. The next subsections will present the system representation using the impedance method and will emphasize the relationship between the system model and the control blocks of the VSC presented in Figure 1.

In a hypothetical situation, the analysis starts with two radial feeders that can be interconnected at the ends of the distribution lines, as shown in Figure 2, with each impedance for each section/node. Terminal voltages V_1 and V_2 represent the loop interconnections.

If we are not interested in the load flow behavior and the values of each voltage node in this system, it is possible to obtain an equivalent representation, as shown in Figure 3, using Thevenin's representation for each distribution feeder, where V_A and V_B are the main feeder voltage sources, T_A and T_B are the main step-down transformers, Z_{L1} and Z_{L2} are the distribution line impedances, Z_1 and Z_2 are load impedances, L_{F1} and L_{F2} are the converter switching filter inductances, T_S is the coupling transformer, and C_{dc} is the series converter DC-link capacitance. V_1, V_2, and V_T are the terminal voltages and the converter's imposed voltages, respectively.

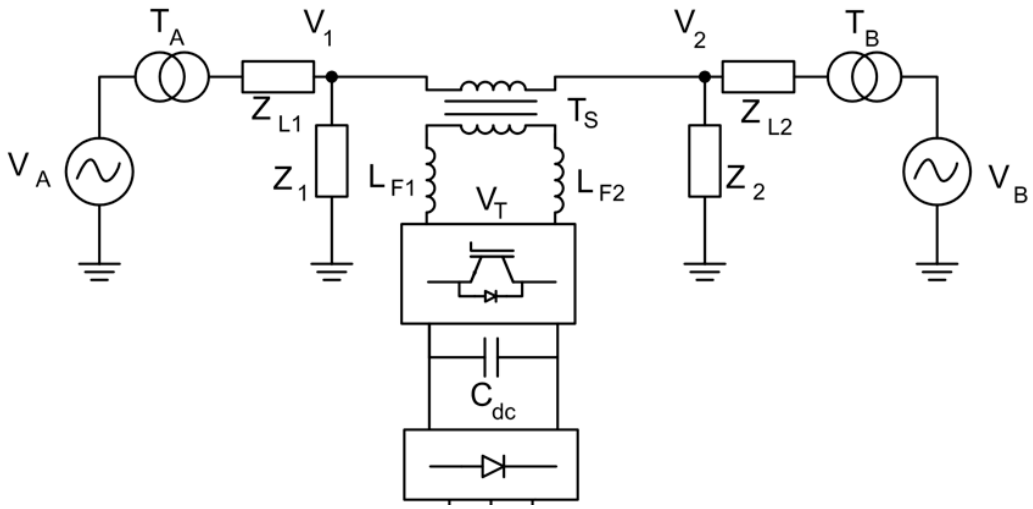

Figure 3. Simplified distribution power system with the series VSC.

Since the converter DC-link has a fixed voltage, as it is maintained by a three-phase diode rectifier connected to one of the feeders (Figure 1), the VSC series can be represented by a controlled AC voltage source, as shown in Figure 4. Figure 4 also shows the conversion to equivalent impedances of the main step-down transformers (Z_{TA} and Z_{TB}), the filter inductances (Z_{F1} and Z_{F2}), and the coupling transformer equivalent impedances (Z_{S1} and Z_{S2}).

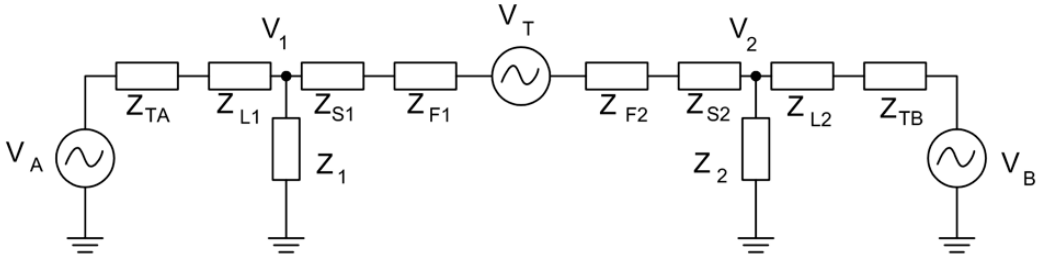

Figure 4. Model considering all system parameters.

The simplified representation can be derived from Figure 5 with the loads represented as current sources (i_{k1} and i_{k2}) as a function of the terminal voltages V_1 and V_2 and the load impedances (i.e., $i_{k1} = V_1/Z_1$ and $i_{k2} = V_2/Z_2$). Additionally, the equivalent transformer

models can be added to the line parameters for further simplification. Figure 5 shows the reduced model where $Z_A = Z_{L1} + Z_{TA}$, $Z_B = Z_{L2} + Z_{TB}$ and $Z_T = Z_{S1} + Z_{F1} + Z_{S1} + Z_{F2}$.

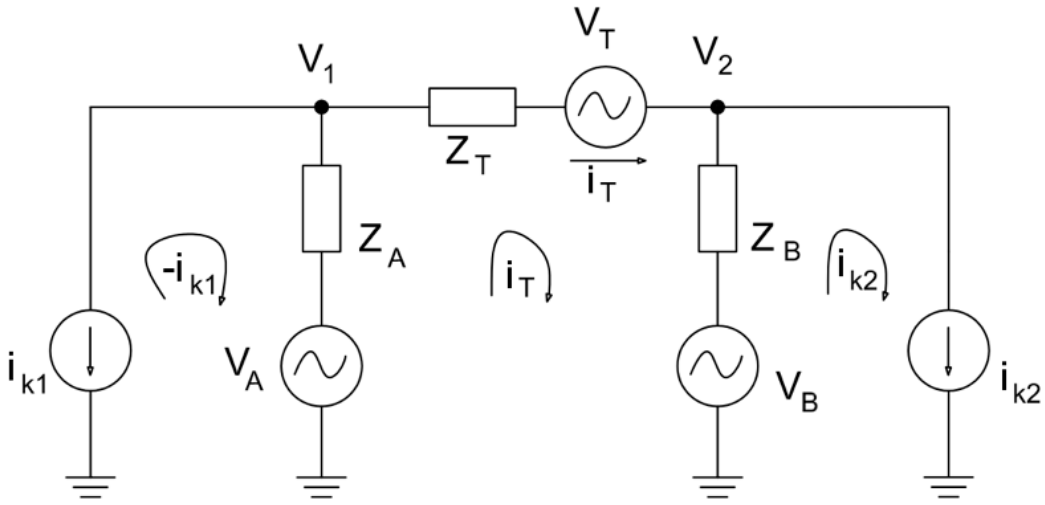

Figure 5. VSC controlled voltage source representation with loads as current sources.

The simplified model of the system and the load behavior provides terminal voltage variations where the controllers should track and compensate for the voltage difference. Therefore, modeling depends on the voltages in the feeders, the line parameters, the coupling transformer parameters, and the filter inductances of the series VSC.

Thus, one must know the current I_T and the behavior of the terminal voltage difference $V_1 - V_2$ under load variance disturbances to model the system as seen by the converter.

From Figure 5, Equation (1) presents the model for the series converter on the AC side as follows:

$$i_{k1}Z_A + I_T(Z_A + Z_B + Z_T) - i_{k2}Z_B = V_A - V_B + V_T \tag{1}$$

Then, the current flowing through loop I_T is derived in (2) as a function of the imposed voltage of the converter. The voltage drop, the loop impedance, or the power transfer between nodes V_1 and V_2 should be adjusted electronically by the converter controllers.

$$I_T = \frac{V_A - V_B + V_T - i_{k1}Z_A + i_{k2}Z_B}{Z_A + Z_B + Z_T} \tag{2}$$

Considering that there is no significant amplitude or phase difference in the main feeders (since they come from the same HV source) their voltage difference can be disregarded, so,

$$V_A - V_B = 0 \tag{3}$$

resulting in Equation (4),

$$I_T = \frac{V_T - i_{k1}Z_A + i_{k2}Z_B}{Z_A + Z_B + Z_T} \tag{4}$$

which can be rewritten as (5)

$$I_T = \underbrace{\frac{V_T}{Z_A + Z_B + Z_T}}_{a} - \underbrace{\frac{i_{k1}Z_A}{Z_A + Z_B + Z_T}}_{b} + \underbrace{\frac{i_{k2}Z_B}{Z_A + Z_B + Z_T}}_{c} \tag{5}$$

From (5) we have three transfer functions. The first represents the imposed voltage influence of the series VSC (a). The second (b) and third (c) terms represent the disturbances in I_T caused by the load variances (i_{k1} and i_{k2}), as shown in Figure 6.

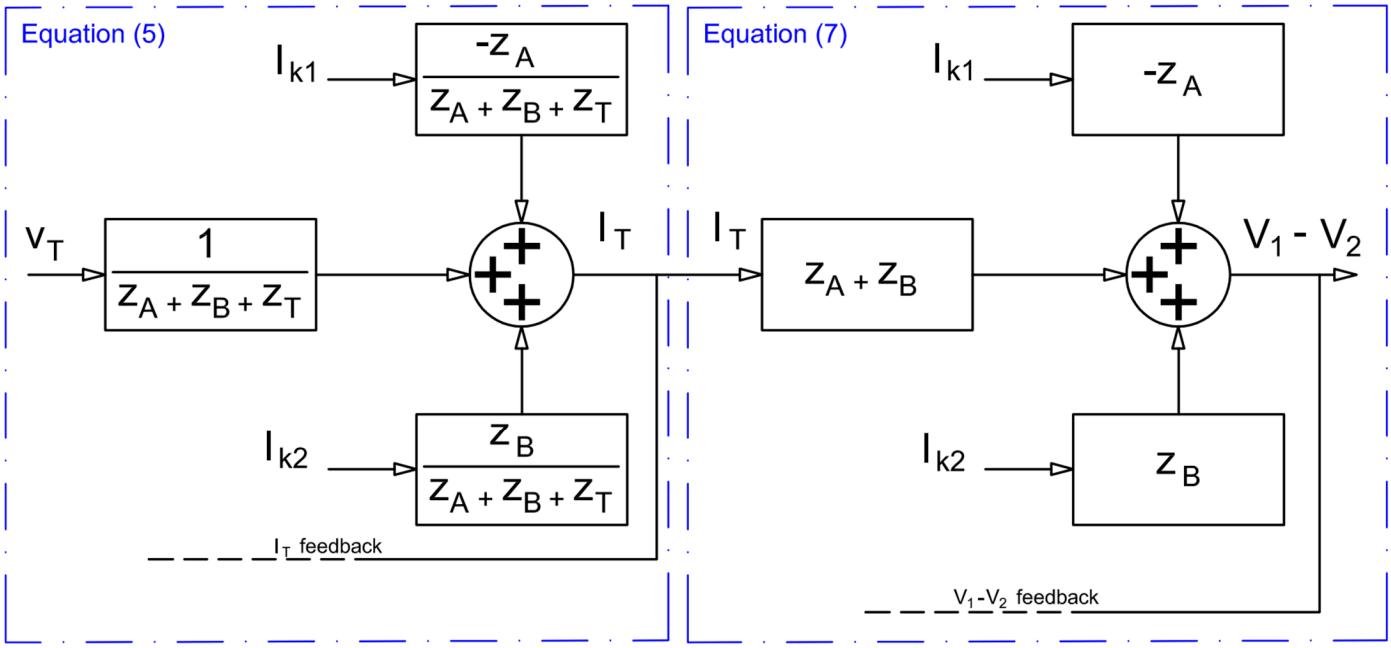

Figure 6. Complete system representation used in the controllers with load disturbances.

To model the complete system that will be controlled with the cascaded P.I. controllers from Figure 1, one must know the behavior of the terminal voltage difference $V_1 - V_2$. So, Equation (6) can be derived from the converter branch of Figure 5,

$$V_1 - V_2 = V_T - I_T Z_T \tag{6}$$

using (4) and (6), we have,

$$V_1 - V_2 = I_T(Z_A + Z_B) + I_{k1} Z_A - I_{k2} Z_B \tag{7}$$

From (7), the block diagram representation is derived in Figure 6. Equation (7) is the relation $(V_1 - V_2)/I_T$ symbolizing the current flowing through loop (I_T) as a function of the terminal voltage difference ($V_1 - V_2$) also considering the load variance as disturbances (Figure 6).

Figure 6 shows the complete system representation seen by the controllers with the load disturbances that include both connected system representations.

Using the Laplace transform, the relationship I_T/V_T and $(V_1 - V_2)/I_T$ can be derived in (8) and (9) from Equations (4) and (7) (disregarding the load disturbance parameters). Equations (8) and (9) describe the dynamics of the system using the proposed control strategy.

The load impedances are much higher than the line impedances, and in part, the load behavior does not cause influences in the control tuning. Disregarding the disturbances in the load behavior, the main transfer functions that represent the system dynamics using the series converter can be derived.

$$\frac{I_T}{V_T} = \frac{1}{(L_A + L_B + L_T)s + (R_A + R_B + R_T)} \tag{8}$$

$$\frac{V_1 - V_2}{I_T} = (L_A + L_B)s + (R_A + R_B) \tag{9}$$

4. Control

The proposed control strategy uses the I_T current and the voltage difference $V_1 - V_2$ as feedback variables. The proposed converter controller is based on the MSRF [36] technique, as presented in Figure 1, and the AC system variables are converted into continuous

variables (V_d and V_q for $V_1 - V_2$) and (i_d and i_q for I_T for the feedback, synchronized with V_1 (by the MSRF-PLL [36]), to be used in the cascaded PI controllers (for d and q axis).

When there are load variance disturbances, the voltage above the converter rises, and the controllers track the voltage difference by transferring the current between both feeders to improve the best voltage profile.

Typical distribution line impedances (Z_A and Z_B) are more than two times the impedance of the L filter of the converter and the coupling transformer equivalent impedance Z_T for the proposed small-rated converter. Thus, the control dynamics are strongly dependent on the line parameters. Additionally, the greater the X/R line ratio, the greater the coupling of variables i_d and i_q. In this case, an additional decoupling technique is needed.

It should be noted that (8) and (9) are first-order transfer functions and the system models previously presented must be converted to a DQ-frame to be analyzed in the P.I.-based controllers.

The main control strategy (current control) is shown in Figure 7, which alone can choose the desired power transfer. Thus, i_d and i_q are the active and reactive currents, respectively. The current control (derived from Figure 1) composed of two P.I. controllers that track the current transfer (i_d and i_q) is compared to the reference values (i_{dref} and i_{qref}) generating the control signals (modulation indexes (mi_d and mi_q), which are multiplied by unity vectors sin (ωt) and cos (ωt) that are added to provide the voltage reference signal V_{pwm} for the unipolar PWM. Furthermore, the outputs from the P.I. controllers (of the current controllers) have saturation limiters (mi_{qmin}, mi_{qmax}, mi_{dmin}, and mi_{dmax}) defined between +1 and −1. The current reference values also have limiters ($i_{drefmin}$, $i_{drefmax}$, $i_{qrefmin}$, and $i_{qrefmax}$) which are defined based on the converter's power rating.

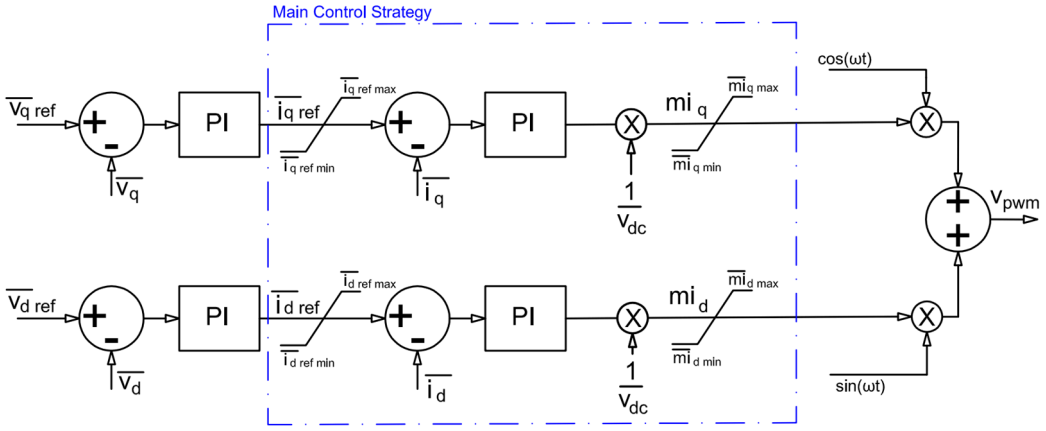

Figure 7. Control strategy.

The outer control loops (voltage control) of Figure 7 are used to track the desired terminal voltage difference ($V_1 - V_2$), also obtained using MSRF by generating the current references (i_{dref} and i_{qref}) comparing V_d and V_q with the desired reference values V_{dref} and V_{qref}.

This control strategy can be used to maintain either a fixed voltage drop at the interconnection point, a fixed series impedance, or to track a zero impedance using the terminal voltage difference references V_{dref} and V_{qref}. The current control P.I. gains are set to be faster than the voltage control in Figure 7.

The modeling method and the MSRF-based control strategy presented in this study can be used as a basis for alternative control purposes, which can be either expanded or changed. For example, one can use impedance compensation, harmonic isolation, voltage restoring, decoupling, SSR mitigation, system identification, techniques, etc., depending on the purpose of each implementation.

When lines of both feeders have similar impedance values, the best choice for the control is to track the zero impedance or the zero voltage drop at the interconnection point provided by the current transfer between them.

5. Prototype

Figure 8 shows a picture from the Medium Voltage Laboratory. The series VSC tests used voltage transformers (VTs, #1), current transformers (CTs, #2), and coupling transformers (#3).

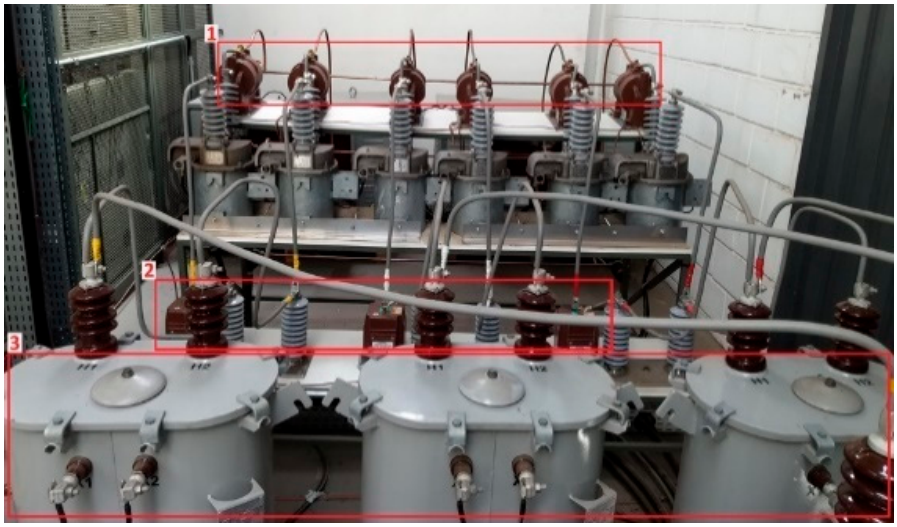

Figure 8. Medium voltage laboratory used in the tests.

Figure 9 shows a picture of the internal electronics composed of three single-phase full-bridge converters (indicated as #1). Basically, this equipment comprises 3 single-phase 37.5 kVA 3:1 coupling transformers, and three independent full-bridge DC-AC converters, with a 500 kVA power transfer capacity.

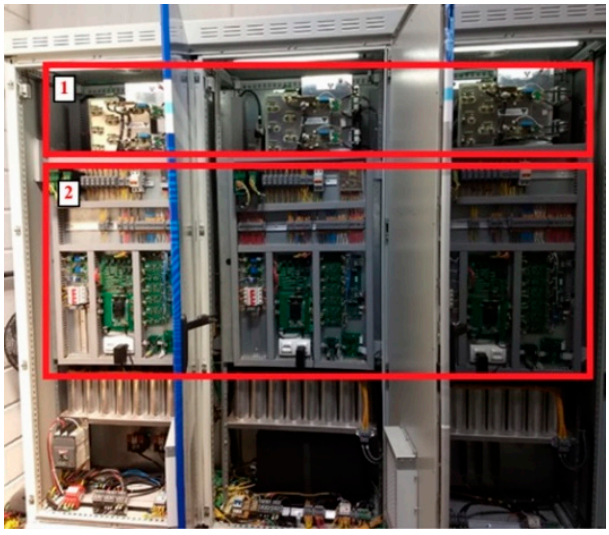

Figure 9. Inner electronics of the series VSC.

Figure 9 also shows the #2 control system, which includes Hall effect transducers, relay command PCB (printed circuit board), a DSP TMS320F28335, analog signal conditioners, and IGBT drivers. Figure 10 shows a picture of the series VSC prototype in a field installation with a view of the developed prototype under test.

Figure 10. Developed three-phase series converter in outdoor installation—13.8 kV field test.

6. Experimental and Simulation Results

This section presents the results for two situations:

1. Tests performed in a three-phase 13.8 kV substation laboratory together with simulation results;
2. Field tests performed in an actual 13.8 kV distribution grid.

The laboratory tests were performed twice, first in a radial configuration, without the series VSC, and then in a meshed configuration, with the series VSC manipulating the power flow, as shown in Figure 11. Additionally, the simulation results will be presented with the same control tuning parameters and the same power system parameters for comparison, using the Matlab® software (version 2019b, licensed for UNIFEI at Itajuba, Brazil).

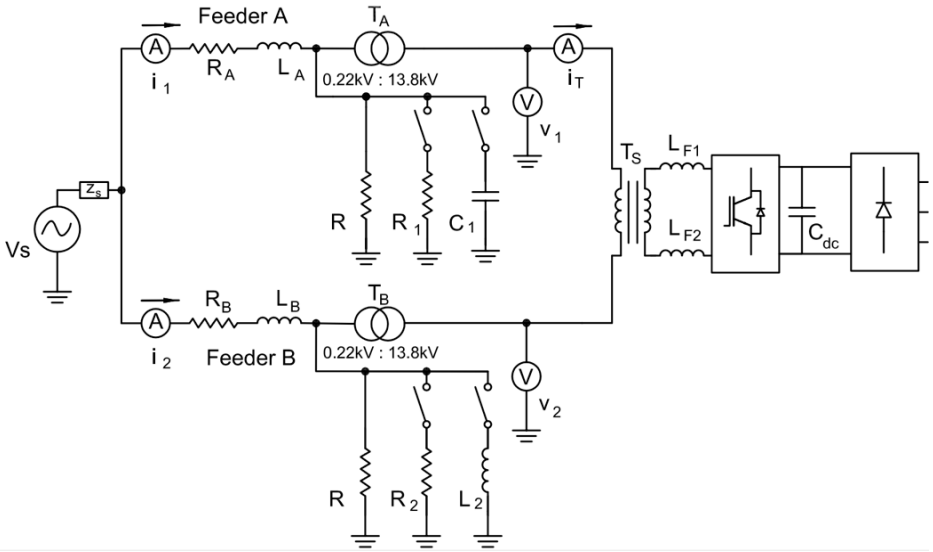

Figure 11. Single-line laboratory test setup diagram.

Figure 11 shows the performed lab test in which the line impedances on the low-voltage side (R_A, L_A, R_B, and L_B), the step-up transformers (T_A and T_B), and the test loads (R, R_1, R_2, C_1, and L_2) with the series VSC interconnecting both ends of the feeders using a coupling transformer T_S. As shown in Figure 1, each phase of the series VSC comprises a

three-phase diode rectifier, a DC-link capacitor (C_{dc}), a low-voltage IGBT-based H-bridge, and an inductive switching filter (L_{F1} and L_{F2}).

The results will present measurements from the beginning of both feeders (using V_S, i_1, and i_2 from Figure 11) and from terminal voltages V_1 and V_2. Additionally, the terminal voltage V_1 and the transferred current I_T, will be used to show the P&Q transfer between the feeders. The measurements were made using power quality meters (Fluke 435) and the sampling period was every 0.5 s. Additionally, the load transitions were performed every 3 min. Table 1 shows the parameters of the converter, the lines, and the loads used in the lab experimental results.

Table 1. Test setup.

Feeders	Three-Phase Loads	Converters
R_A = 0.6 Ω	R_1 = 12 Ω	L_{F1} = 250 µH
L_A = 530 µH	R_2 = 12 Ω	L_{F2} = 250 µH
R_B = 0.5 Ω	C_1 = 7 kVAr	C_{dc} = 6666 µF
L_B = 530 µH	L_2 = 12 kVAr	
	R = 12 kW	

In addition, the simulation results will show the behavior of the system in a meshed configuration with the series VSC operation. Furthermore, for less computational effort, the simulation load transitions were performed every 15 s resulting in a 60 s simulation test.

The data for the transformers used in the test setup are presented in Table 2. Respectively, T_A, T_B, and T_S are the step-up transformers and the coupling transformer.

Table 2. Transformer setup.

Transformer Data		Z%	r_1	x_1	r_2	x_2
T_A, T_B	66.0 kVA 0.22:13.8 kV	6%	0.013	0.043	51.15	168.6
T_S	37.5 kVA 600:1800 V	5.3%	0.06	0.26	0.54	2.34

Table 3 shows the gains of the P.I. controllers defined by the control strategy.

Table 3. Control setup.

Current Control		Voltage Control	
Kp_d = 10	Kp_q = 0.8	Kp_{vd} = −0.000003	Kp_{vq} = −0.000001
Ki_d = 100	ki_q = 120	Ki_{vd} = 180	ki_{vq} = 800

6.1. Active Power Behavior

The first tests show the system behavior with resistive loads controlling the active power transfer between the feeders. The tests used five resistive load transition stages as follows:

1. Initial condition;
2. R_1 insertion;
3. R_1 removal;
4. R_2 insertion;
5. R_2 removal.

Figure 12a shows the terminal voltages (V_1 and V_2) for both the radial (without the series VSC) and meshed configurations (with the series VSC manipulating the power flow). One should note that the series converter improves the voltage profile of the overloaded feeder while it decreases the voltage of the less loaded feeder, which converts the interconnected terminal voltages into an intermediate value via power transfer. It also shows that the main feeder V_s also undergoes smaller voltage variations.

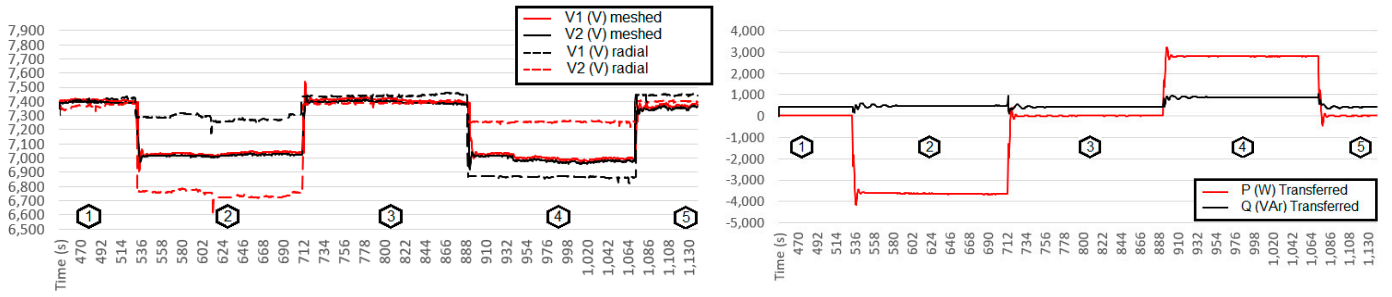

(**a**) (**b**)

Figure 12. Behavior of the phase-to-ground terminal voltages and the power flow; (**a**) V_1 and V_2; (**b**) transferred P and Q.

Figure 13a,b show the terminal voltage's behavior and the transferred power flow in the simulation results which demonstrate equivalence when compared with experimental results.

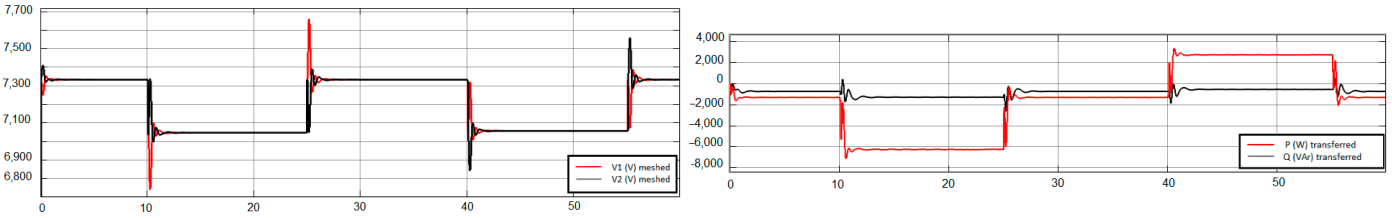

(**a**) (**b**)

Figure 13. Simulation results with the series VSC operation; (**a**) V_1 and V_2; (**b**) transferred P and Q.

For the radial configuration, in stage 2 (i.e., R_1 insertion) the feeder A terminal voltage V_1 drops from 7.4 kV to 6.4 kV and the feeder B terminal voltage V_2 also drops but slightly less than the first.

In stage 3, R_1 was removed, returning the whole system to the initial voltage conditions. In stage 4, the inserted R_2 shows a V_2 voltage drop less than in stage 2 because feeder B is stronger than feeder A.

Stage 5 ends the resistive test by removing load R_2 that returns the terminal voltages to the initial voltage conditions.

Figure 12b shows the active and reactive power values transferred in the loop. Stage 2 (R_1 insertion) shows the transferred power from feeder B to feeder A, which consequently improves the terminal voltages by an intermediate value via power transfer. Stage 4 (R_2 insertion), shows the power transfer from feeder A to feeder B, also improving the terminal voltages more than in the radial configuration. This shows the power transfer levels achieved from the series converter tracking the best terminal voltage profiles in the interconnected feeders.

Figure 14a shows the phase graph for the stage 2 load transition, which shows that the inserted resistive loads had only voltage magnitude changes without phase angle variation in a radial configuration for these distribution line parameters.

In a meshed configuration, Figure 14b shows that the phasors in stage 2, with current I_T approximately 180° from both terminal voltages, equal the same values after the power transfer, i.e., the flow from feeder B to Feeder A. It shows that the converter always tracks the best terminal voltage profile, consequently alleviating the overloaded feeder.

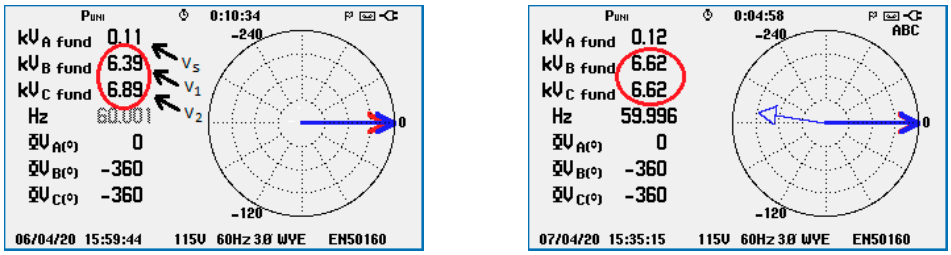

(**a**)

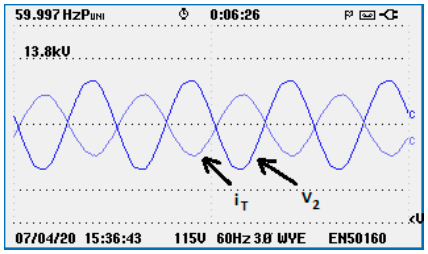

(**b**)

Figure 14. Phasors before and after power flow manipulation; (**a**) R_1 insertion stage–without the converter operation; (**b**) R_1 insertion stage–with the converter operation.

Figure 15a,b show the active power delivered by each feeder and the loading balance provided by the converter power flow manipulation.

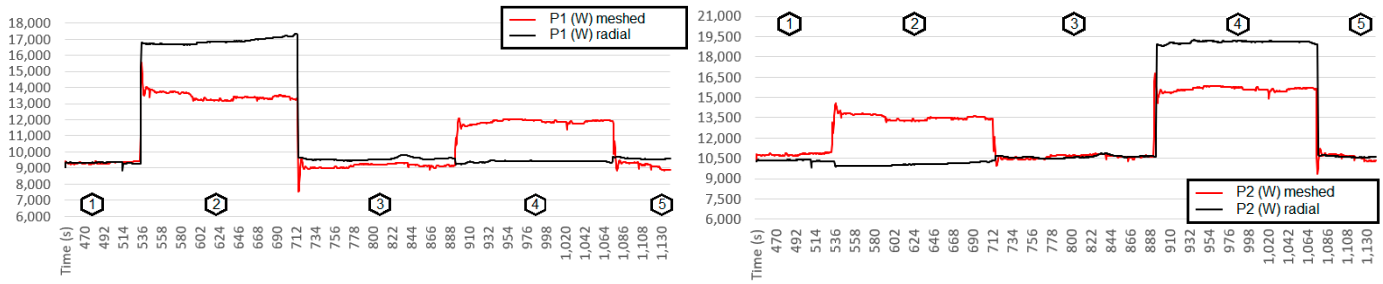

(**a**) (**b**)

Figure 15. Active power delivered by each feeder; (**a**) P provided from feeder A; (**b**) P provided from feeder B.

Figure 16a,b present the active and reactive power delivered by the feeders for the simulation. The reactive power shown in simulation results provides the information that only resistive loads were inserted in this test. To make a clear view, the experimental results do not show the measurement of reactive power in the test with resistive loads.

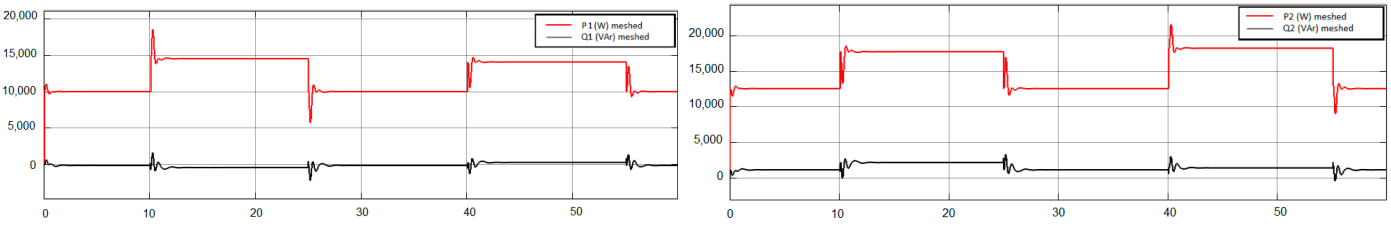

(**a**) (**b**)

Figure 16. Simulation results for active and reactive power delivered by each feeder; (**a**) P and Q provided from feeder A; (**b**) P and Q provided from feeder B.

As shown in Figure 17a,b, we noted that there is a larger voltage variation (voltage sag and swells) during load transitions in the respective feeder where the load was inserted. Thus, the converter uses slow dynamics to achieve a variable impedance during load insertions, feeding the other branch slowly, and these dynamics can be selected when tuning the voltage controller.

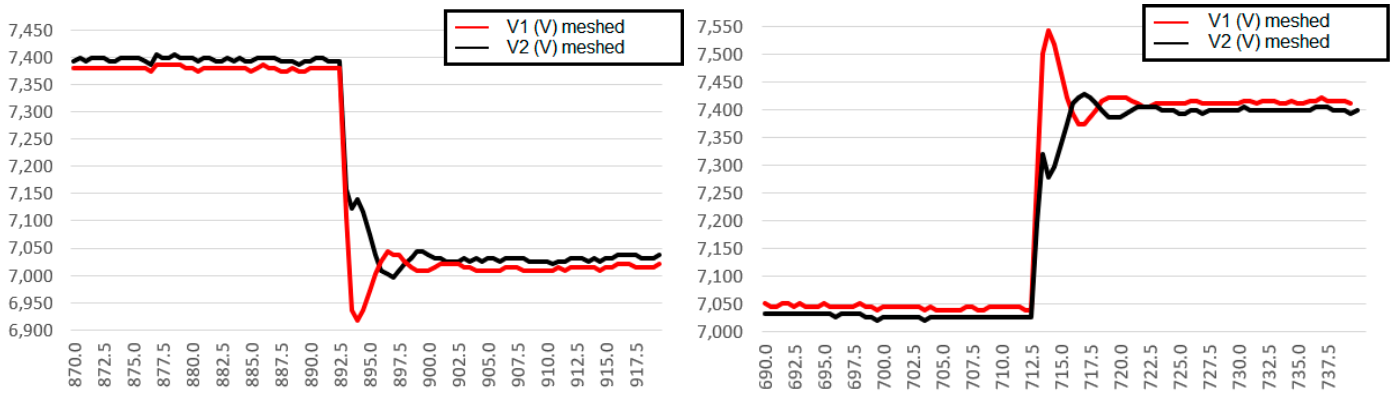

(**a**) (**b**)

Figure 17. Terminal voltage dynamics with the series VSC; (**a**) R_1 insertion; (**b**) R_1 removal.

Additionally, instead of the behavior observed for physical interconnections, there are partial voltage sags in the series VSC occurring at the respective feeder where the load was inserted, as shown in Figure 17a. Regarding the swells shown in Figure 17b, we noted a predominant swell when load R_1 was removed.

In conclusion, when the series converter transfers power between the feeders, the loading is distributed autonomously, and the emptier feeder always feeds the loaded feeder.

6.2. Reactive Power Behavior

In order to reproduce reactive power manipulation using the series converter, the inductive and capacitive loads were inserted in this test. These results also have five stages, as follows:

1. Initial condition;
2. L_2 insertion;
3. C_1 insertion;
4. C_1 removal;
5. L_2 removal.

Figure 18a shows the terminal voltage behavior for both meshed and radial converter operations. Although reactive compensation does not significantly improve the voltage profile in the distribution lines, it reduces the current flowing through the lines, thus reducing technical losses. The radial configuration shows that the terminal voltages drop less than in the resistive load test, and the main feeder V_S also experiences small voltage variations because of the impedance Z_S effect (Figure 11).

Figure 19a,b shows the same simulation results which also demonstrate equivalence when compared with experimental results.

In stage 2 (i.e., L_2 insertion), the terminal voltage V_2 drops, and the terminal voltage V_1 also drops but slightly less. In stage 3, C_1 was inserted, which slightly improved the terminal voltage profile. In stage 4, C_1 was removed, returning to the voltage condition in stage 2, with only L_2 inserted. Finally, stage 5 showed the initial voltage profile. Figure 18b presents the active and reactive power transfer from the series converter, which shows predominant reactive power manipulation for the same control strategy. The small active power is provided via losses in the line parameters and via the reactive loads, which are also simultaneously manipulated.

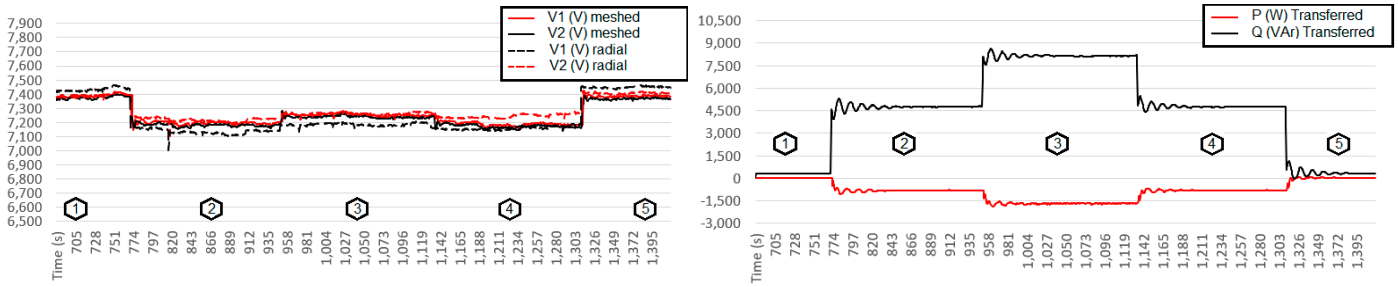

(**a**) (**b**)

Figure 18. Phase-to-ground terminal voltages behavior and power flow; (**a**) V_1 and V_2; (**b**) transferred P and Q.

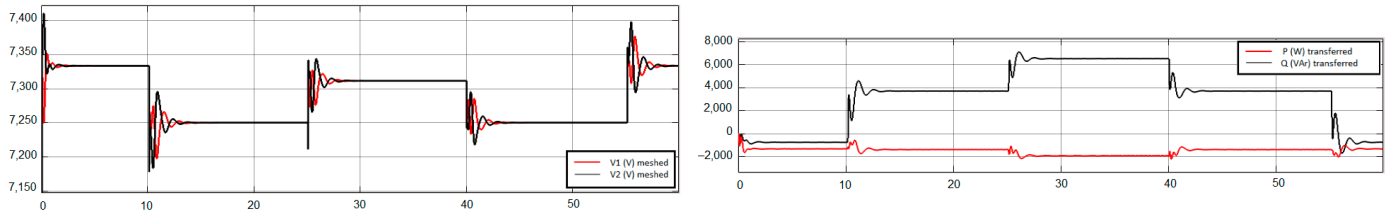

(**a**) (**b**)

Figure 19. Simulation results of phase-to-ground terminal voltages behavior and the power flow with the converter operation; (**a**) V_1 and V_2; (**b**) transferred P and Q.

Figure 20a presents the phase graph for stage 3, which shows that, without the radial converter operation for these distribution line parameters, inserted reactive loads show predominant phase angle variations. Figure 20b shows the state of stage 3 with the series converter transferring power to compensate for the achieved phase angle difference via the reactive loads. Additionally, one should note that in stage 3 capacitor C_1 is inserted into feeder A, and inductance L_2 is inserted into feeder B, to compensate for the inductive reactive power of both feeders using the series converter.

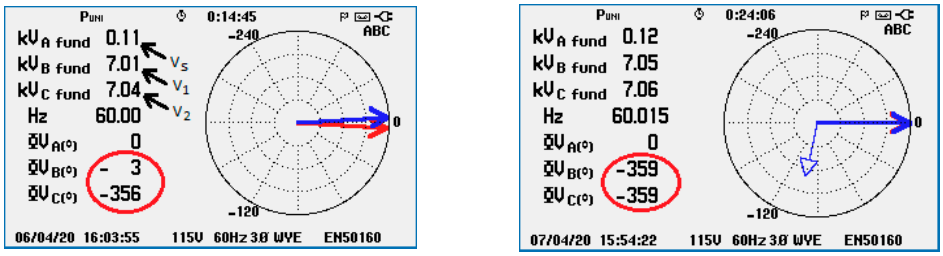

(**a**)

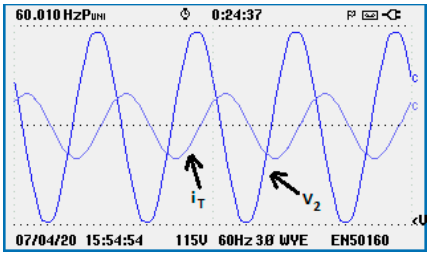

(**b**)

Figure 20. With and without converter operation voltage analysis; (**a**) C_1 insertion stage–without the converter operation; (**b**) C_1 insertion stage–with converter operation.

With respect to stage 3, Figure 20b shows a higher current transfer from feeder A to feeder B to compensate for the higher terminal voltage angular difference provided by inserting loads L_2 and C_1. It also shows current I_T-90° from the equalized terminal voltages.

Figure 21a,b show the behavior of the reactive powers from the feeders for both converter operations. One should note that, when capacitance C_1 was inserted (stage 3), the provided reactive power was reduced in both feeders. Consequently, this results in a reduced reactive power requirement from the main source V_S (Figure 11) with the converter operation, ZS and V2chuit Boardbances in damentals resulting in technical loss reductions when both radial feeders are interconnected using the series converter power flow manipulation.

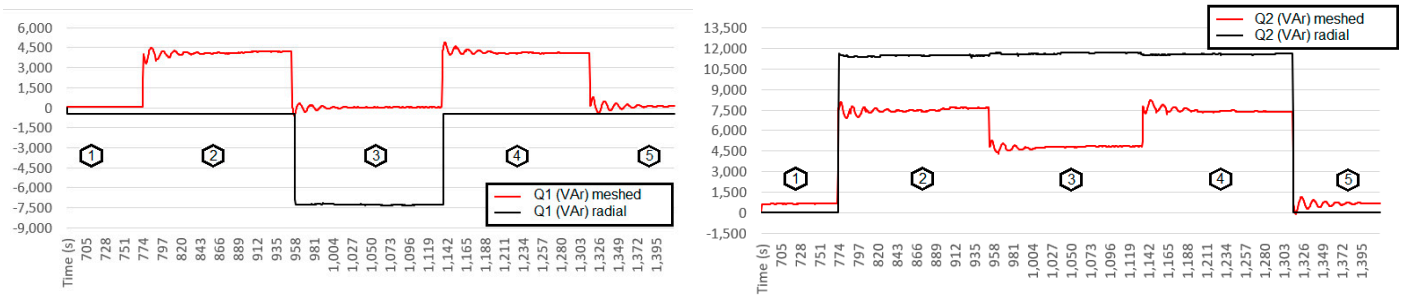

(**a**) (**b**)

Figure 21. Reactive power delivered by each feeder; (**a**) Q provided by feeder A; (**b**) Q provided by feeder B.

Figure 22a,b show the simulation results. The constant active power presented in the simulations shows that only reactive loads were inserted/removed in this test, but a constant load R is maintained in both feeders (Figure 11) during the reactive load transitions.

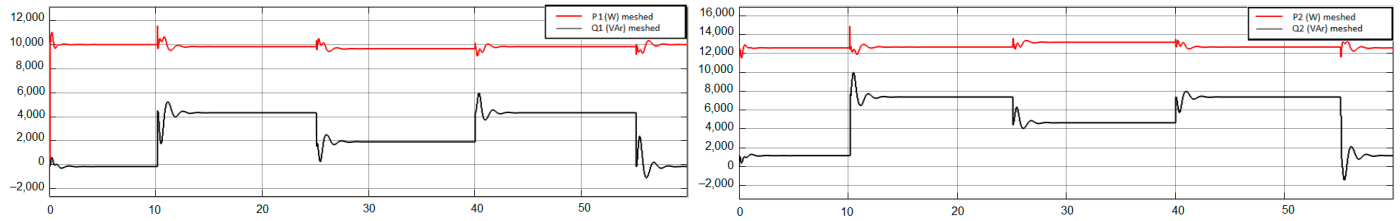

(**a**) (**b**)

Figure 22. Simulation results for P and Q delivered by each feeder; (**a**) P and Q provided by feeder A; (**b**) P and Q provided by feeder B.

Thus, the series VSC, with inserted capacitance C_1 in feeder A, compensates for the reactive inductance present in feeder B, provided by L_2 with the same control strategy that takes decisions looking at the behavior of the terminal voltages.

In addition, simulations presented together with laboratory tests show comparable and converging results for both active and reactive power behaviors validating the proposed approach.

Finally, Figure 23 shows the power factor measurements showing reductions in reactive power requirements from both feeders when the radial system is changed to a meshed feeder with a series VSC.

Sections 6.1 and 6.2 also showed simulation results that could be analyzed in a comparative way with the experimental results performed in the laboratory. The simulations presented transient voltage and power oscillations shorter than the experimental results, caused by the uncertainties of the actual modeling parameters. However, observing the

results as a whole, the agreement between the simulation and experimental tests could validate the equivalence of the computational representation and reality, showing that the proposed converter can effectively improve the voltage profile by properly controlling active and reactive power flow, both in simulation and experimental tests.

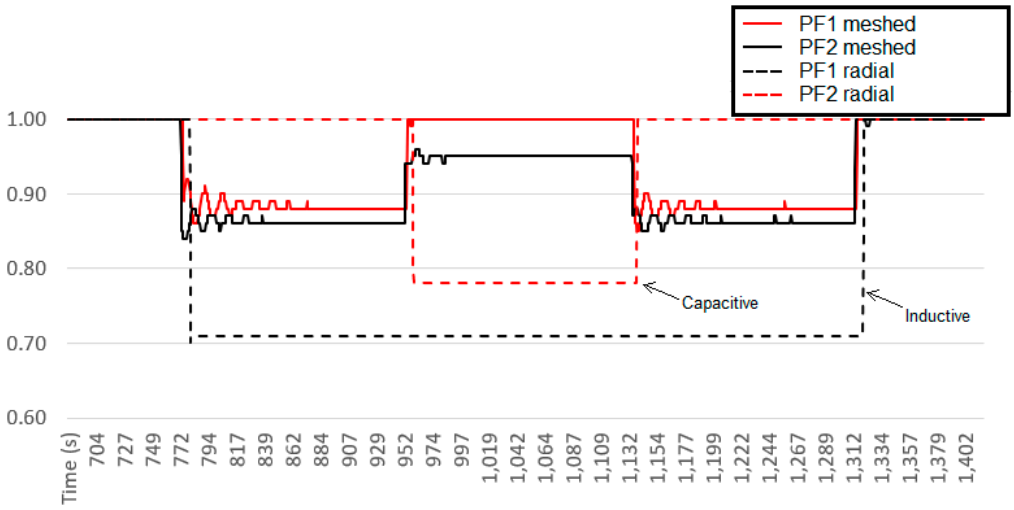

Figure 23. Power factor measurements at the beginning of feeders A and B.

6.3. Field Test

The field test was performed using only the current control shown in Figure 7, by means of manual increments of active and reactive current references (i_{dref} and i_{qref}). Figure 24 presents the *P* and *Q* measurements during the field test.

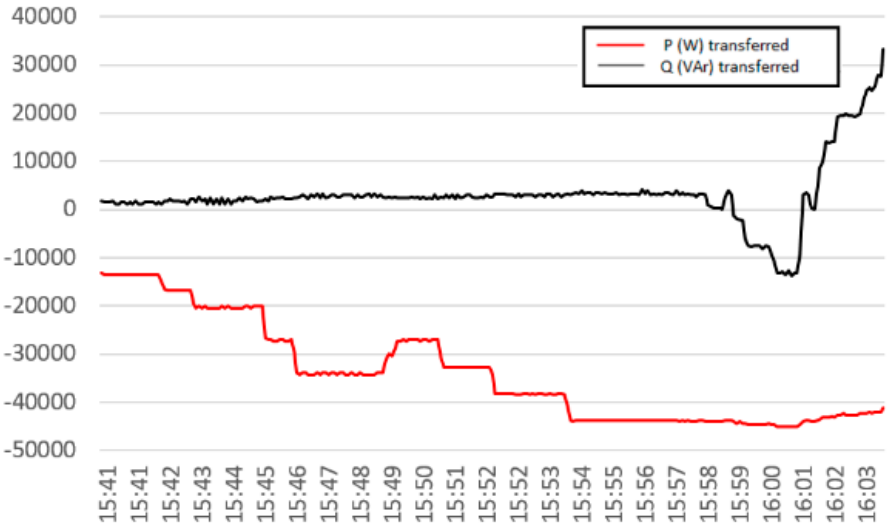

Figure 24. Field test—P and Q transferred between the feeders for phase A.

At the beginning, the reactive power reference was maintained at 0 VAr while the active power was changed in small steps. After 15:57 (indicated in Figure 24), the active power was fixed at approximately 45 kW while the transferred reactive power was manipulated in both directions showing the independent P and Q manipulation for the proposed control strategy, validating the presented formulations of this study also in a real field system.

7. Conclusions

Nowadays, a way of managing the power flows in real time using smart methods is needed. The presented approach is for application in medium voltage distribution grids

and the proposed converter showed a solution installed at 13.8 kV voltage levels which shows the independent control of active and reactive power flow. Because of the typical small phase difference of terminal voltage in distribution grids, the hardware power rating is only a small fraction of the total power that it can handle (in this case, 20%). So, a series VSC, which comprises three independent single-phase converters, is a cost-effective solution for accomplishing active and reactive power flow control in this scenario.

This series VSC solution provides capacity increase for the growth of loads in distribution feeders and the increased use of distributed generation that requires new investments in infrastructure to mitigate these contingencies. One of the contributions refers to the conversion of a traditional radial distribution grid into a permanent meshed grid in a secure way. Additionally, it can be extensively installed in actual distribution grids for power quality improvements and real-time power manipulation, providing an operation that can be either autonomous or remotely controlled by an operator.

This study presented the modeling fundamentals, a control proposal based on MSRF using a series voltage source converter for medium voltage distribution grids (13.8 kV). Thus, the presented formulations were validated with simulations and experimental results in a lab environment and actual distribution system. The results showed improvement in the terminal voltage profile, enhancing the whole system behavior under load variance disturbances, thus proving the applicability of the developed solution without instabilities.

Author Contributions: Conceptualization, G.L.-T. and J.S.-F.; writing, G.G.P.; formal analysis and investigation, C.H.d.S. and G.G.P.; methodology, R.B.G., R.R.P. and W.C.S.; performed tests, control software development, and hardware assembly, B.P.B.G., G.G.P., C.H.d.S., R.B.G., R.R.P. and W.C.S.; experiments supervision, R.B.G., R.R.P. and G.L.-T.; material resources, J.S.-F. All authors have read and agreed to the published version of the manuscript.

Funding: This research received no external funding.

Institutional Review Board Statement: Not applicable.

Informed Consent Statement: Not applicable.

Data Availability Statement: Not applicable.

Acknowledgments: The authors would like to thank the following Brazilian Research Agencies CNPq, CAPES, FAPEMIG, and ANEEL Research and Development for the support of this project.

Conflicts of Interest: The authors declare no conflict of interest.

Abbreviations

The following abbreviations are used in this manuscript:

SSSC	Static Synchronous Series Compensator
VSC	Voltage Source Converter
FACTS	Flexible AC Transmission Systems
DG	Distributed Generation
MSRF	Modified Synchronous Reference Frame
RACDS	Resilient AC Distribution Systems
DSP	Digital Signal Processor
DVR	Dynamic Voltage Restorer
PST	Phase Shift Transformer
IGBT	Insulated Gate Bipolar Transistor
UPFC	Unified Power Flow Controller
CD-PAR	Compact Dynamic Phase Angle Regulator
DSSSC	Distribution Static Synchronous Series Compensator
CNT	Controllable Network Transformer
BTB	Back-to-Back
SCADA	Supervisory Control and Data Acquisition

References

1. Gasperic, S.; Mihalic, R. The Impact of Serial Controllable FACTS Devices on Voltage Stability. *Int. J. Electr. Power Energy Syst.* **2015**, *64*, 1040–1048. [CrossRef]
2. Gandoman, F.H.; Ahmadi, A.; Sharaf, A.M.; Siano, P.; Pou, J.; Hredzak, B.; Agelidis, V.G. Review of FACTS Technologies and Applications for Power Quality in Smart Grids with Renewable Energy Systems. *Renew. Sustain. Energy Rev.* **2018**, *82*, 502–514. [CrossRef]
3. Ordóñez, C.A.; Gómez-Expósito, A.; Maza-Ortega, J.M. Series Compensation of Transmission Systems: A Literature Survey. *Energies* **2021**, *14*, 1717. [CrossRef]
4. Imdadullah; Amrr, S.M.; Asghar, M.S.J.; Ashraf, I.; Meraj, M. A Comprehensive Review of Power Flow Controllers in Interconnected Power System Networks. *IEEE Access* **2020**, *8*, 18036–18063. [CrossRef]
5. Hingorani, N.G. High Power Electronics and Flexible AC Transmission System. *IEEE Power Eng. Rev.* **1988**, *8*, 3–4. [CrossRef]
6. Peng, F.Z. Flexible AC Transmission Systems (FACTS) and Resilient AC Distribution Systems (RACDS) in Smart Grid. *Proc. IEEE* **2017**, *105*, 2099–2115. [CrossRef]
7. Hebal, S.; Mechta, D.; Harous, S.; Dhriyyef, M. Hybrid Energy Routing Approach for Energy Internet. *Energies* **2021**, *14*, 2579. [CrossRef]
8. Ilea, V.; Bovo, C.; Falabretti, D.; Merlo, M.; Arrigoni, C.; Bonera, R.; Rodolfi, M. Voltage Control Methodologies in Active Distribution Networks. *Energies* **2020**, *13*, 3293. [CrossRef]
9. Sayed, M.A.; Takeshita, T. All Nodes Voltage Regulation and Line Loss Minimization in Loop Distribution Systems Using UPFC. *IEEE Trans. Power Electron.* **2011**, *26*, 1694–1703. [CrossRef]
10. Sayed, M.A.; Takeshita, T. Line Loss Minimization in Isolated Substations and Multiple Loop Distribution Systems Using the UPFC. *IEEE Trans. Power Electron.* **2014**, *29*, 5813–5822. [CrossRef]
11. Saradarzadeh, M.; Farhangi, S.; Schanen, J.L.; Jeannin, P.-O.; Frey, D. The Benefits of Looping a Radial Distribution System with a Power Flow Controller. In Proceedings of the 2010 IEEE International Conference on Power and Energy, Kuala Lumpur, Malaysia, 29 November–1 December 2010; pp. 723–728.
12. Wang, L.; Feng, S.; Shi, F. Risk Analysis of ClosING Loop Operation Based on the Main and Distribution Network Integration. In Proceedings of the 2012 China International Conference on Electricity Distribution, Shanghai, China, 10–14 September 2012; pp. 1–4.
13. Bacha, S.; Frey, D.; Schanen, J.L.; Lepelleter, E.; Jeannin, P.O.; Caire, R. Short-Circuit Limitation Thanks to a Series Connected VSC. In Proceedings of the 2008 Twenty-Third Annual IEEE Applied Power Electronics Conference and Exposition, Austin, TX, USA, 24–28 February 2008; pp. 1938–1945.
14. Saradarzadeh, M.; Farhangi, S.; Schanen, J.L.; Jeannin, P.-O.; Frey, D. Combination of Power Flow Controller and Short-Circuit Limiter in Distribution Electrical Network Using a Cascaded H-Bridge Distribution-Static Synchronous Series Compensator. *Transm. Distrib. IET Gener.* **2012**, *6*, 1121–1131. [CrossRef]
15. Farmad, M.; Farhangi, S.; Afsharnia, S.; Gharehpetian, G.B. Modelling and Simulation of Voltage Source Converter-Based Interphase Power Controller as Fault-Current Limiter and Power Flow Controller. *Transm. Distrib. IET Gener.* **2011**, *5*, 1132–1140. [CrossRef]
16. Saradarzadeh, M.; Farhangi, S.; Schanen, J.L.; Jeannin, P.-O.; Frey, D. Application of Cascaded H-Bridge Distribution-Static Synchronous Series Compensator in Electrical Distribution System Power Flow Control. *IET Power Electron.* **2012**, *5*, 1660–1675. [CrossRef]
17. Chen, H.; Iyer, A.R.; Harley, R.G.; Divan, D. Dynamic Grid Power Routing Using Controllable Network Transformers (CNTs) with Decoupled Closed-Loop Controller. *IEEE Trans. Ind. Appl.* **2015**, *51*, 2361–2372. [CrossRef]
18. Chen, H.; Iyer, A.; Harley, R.; Divan, D. Decoupled Closed-Loop Power Flow Control for the Controllable Network Transformers (CNT). In Proceedings of the 2014 IEEE Applied Power Electronics Conference and Exposition—APEC 2014, Fort Worth, TX, USA, 16–20 March 2014; pp. 2148–2155.
19. Prasai, A.; Kandula, R.P.; Moghe, R.; Heidel, T.; Schauder, C.; Divan, D. Compact Dynamic Phase Angle Regulator for Power Flow Control. In Proceedings of the 2015 IEEE Energy Conversion Congress and Exposition (ECCE), Montreal, QC, Canada, 20–24 September 2015; pp. 4985–4992.
20. Kandula, R.P.; Prasai, A.; Chen, H.; Mayor, R.; Lambert, F.; Heidel, T.; Schauder, C.; Divan, D. Design Considerations and Experimental Results for a 12.47-KV 3-Phase 1 MVA Power Router. In Proceedings of the 2015 IEEE Energy Conversion Congress and Exposition (ECCE), Montreal, QC, Canada, 20–24 September 2015; pp. 5000–5007.
21. Tamimi, B.; Cañizares, C.; Battistelli, C. Hybrid Power Flow Controller Steady-State Modeling, Control, and Practical Application. *IEEE Trans. Power Syst.* **2017**, *32*, 1483–1492. [CrossRef]
22. Tamimi, B.; Cañizares, C.A. Modeling and Application of Hybrid Power Flow Controller in Distribution Systems. *IEEE Trans. Power Deliv.* **2018**, *33*, 2673–2682. [CrossRef]
23. Cano, J.M.; Norniella, J.G.; Rojas, C.H.; Orcajo, G.A.; Jatskevich, J. Application of Loop Power Flow Controllers for Power Demand Optimization at Industrial Customer Sites. In Proceedings of the 2015 IEEE Power Energy Society General Meeting, Denver, CO, USA, 26–30 July 2015; pp. 1–5.
24. Okada, N. A Method to Determine the Distributed Control Setting of Looping Devices for Active Distribution Systems. In Proceedings of the 2009 IEEE Bucharest PowerTech, Bucarest, Romania, 28 June–2 July 2009; pp. 1–6.

25. Okada, N. Autonomous Loop Power Flow Control for Distribution System. In Proceedings of the Seventh International Conference on AC and DC Transmission, 2001, London, UK, 28–30 November 2001; pp. 150–155.
26. Xing, X.; Lin, J.; Wan, C.; Song, Y. Model Predictive Control of LPC-Looped Active Distribution Network with High Penetration of Distributed Generation. *IEEE Trans. Sustain. Energy* **2017**, *8*, 1051–1063. [CrossRef]
27. Wu, R. Improve the Flexibility of Power Distribution Network by Using Back-to-Back Voltage Source Converter. Ph.D. Thesis, University of Warwick, Coventry, UK, 2018.
28. Weedy, B.M.; Cory, B.J.; Jenkins, N.; Ekanayake, J.B.; Strbac, G. *Electric Power Systems*, 5th ed.; Wiley: Chichester, UK, 2012; ISBN 978-0-470-68268-5.
29. Alcalá, J.; Cárdenas, V.; Aganza, A.; Gudiño-Lau, J.; Charre, S. The Performance of the BTB-VSC for Active Power Balancing, Reactive Power Compensation and Current Harmonic Filtering in the Interconnected Systems. *Energies* **2020**, *13*, 831. [CrossRef]
30. Jiang, F.; Li, Y.; Tu, C.; Guo, Q.; Li, H. A Review of Series Voltage Source Converter with Fault Current Limiting Function. *Chin. J. Electr. Eng.* **2018**, *4*, 36–44. [CrossRef]
31. Bashar, E.; Rogers, D.; Wu, R.; Ran, L.; Jennings, M.; Green, T.C.; Mawby, P. A New Protection Scheme for an SSSC in an MV Network by Using a Varistor and Thyristors. *IEEE Trans. Power Deliv.* **2021**, *36*, 102–113. [CrossRef]
32. Pinheiro, G.; Sant'Ana, W.; Rodrigues Pereira, R.; Bauwelz Gonzatti, R.; Guimarães, B.; Lambert-Torres, G.; da Silva, L.E.; Mollica, D.; Filho, J.; Silva, C.; et al. Comparação de Técnicas de Controle para Bloqueio Harmônico Utilizando um Filtro Ativo Série em Redes de Distribuição. In Proceedings of the XVIII Encontro Regional Ibero-Americano do CIGRÉ, XVIII ERIAC, Foz do Iguaçu, Brazil, 19–23 May 2019. [CrossRef]
33. Ghulomzoda, A.; Gulakhmadov, A.; Fishov, A.; Safaraliev, M.; Chen, X.; Rasulzoda, K.; Gulyamov, K.; Ahyoev, J. Recloser-Based Decentralized Control of the Grid with Distributed Generation in the Lahsh District of the Rasht Grid in Tajikistan, Central Asia. *Energies* **2020**, *13*, 3673. [CrossRef]
34. Dinh, M.-C.; Tran, M.-Q.; Lee, J.-I.; Lee, S.-J.; Lee, C.H.; Yoon, J.; Park, M. Suggestion of a New Protection Scheme for a Transmission System Equipped with a Thyristor-Controlled Series Capacitor. *Energies* **2019**, *12*, 2250. [CrossRef]
35. Hingorani, N.G.; Gyugyi, L. *Understanding FACTS: Concepts and Technology of Flexible AC Transmission Systems*, 1st ed.; Wiley-IEEE Press: New York, NY, USA, 1999; ISBN 978-0-7803-3455-7.
36. da Silva, C.H.; Pereira, R.R.; da Silva, L.E.B.; Lambert-Torres, G.; Bose, B.K.; Ahn, S.U. A Digital PLL Scheme for Three-Phase System Using Modified Synchronous Reference Frame. *IEEE Trans. Ind. Electron.* **2010**, *57*, 3814–3821. [CrossRef]